Some more exact enumeration results for 1D cellular automata

1987 J. Phys. A: Math. Gen. 20 4039

(http://iopscience.iop.org/0305-4470/20/12/049)

J. Phys. A: Math. Gen. **20** (1987) 4039–4046. Printed in the UK

COMMENT

Some more exact enumeration results for 1D cellular automata

Peter Grassberger

Physics Department, University of Wuppertal, Gauss-Strasse 20, D-56 Wuppertal 1, West Germany

Received 28 January 1987

Abstract. We present exact enumeration results for the elementary cellular automaton rules 22, 30, 45 and 120 in Wolfram's notation. Obtained by a new algorithm, they improve previous results considerably. They confirm the existence of 'hidden' power-behaved long-range correlations in the patterns created by these rules.

Cellular automata (CA) [1] are spatially extended dynamical systems with discrete space, discrete time and with discrete variables at each spacetime point. Due to this discreteness, they are extremely easy to simulate and thus represent a very convenient tool for exploring the complexities in the behaviour of non-linear spatially extended systems. The basic surmise thereby is of course that features found in cellular automata can also be found in continuous systems. This hope is based on systems with few degrees of freedom, where complex behaviour is, e.g., much easier to find in maps than in flows, but where the phenomena in both are basically similar.

In this spirit, Wolfram [2] has initiated a systematic study of the simplest CA, called 'elementary' by him: one-dimensional arrays of 'spins' with just two states $s = 0$ and 1, and with deterministic evolutions

$$s_i' = F(s_{i-1}, s_i, s_{i+1}) \tag{1}$$

depending only on nearest neighbours. Here, $F(r, s, t)$ is one of the $2^{2^3} = 256$ Boolean functions of three variables. Wolfram proposed to denote the resulting 256 elementary CA rules by the number obtained by regarding the array of eight bits

$$\{F(1,1,1),\ F(1,1,0),\ F(1,0,1), \ldots, F(0,0,0)\}$$

as its binary representation. Thus, for example, the rule

$$s_i' = \begin{cases} 1 & \text{if exactly one of } s_{i-1},\ s_i \text{ and } s_{i+1} \text{ is } 1 \\ 0 & \text{otherwise} \end{cases}$$

becomes rule $[00010110]_2 = 22$, while $s_i' = (s_{i-1}\ \text{XOR}\ s_{i+1})$ is rule 90, and $s_i' = (s_{i-1}\ \text{XOR}\ s_{i+1})\ \text{AND NOT}\ s_i$ is rule 18.

In the following, we shall be interested in the long-time behaviour of elementary CA, following from random initial conditions on infinite lattices.

It was found in [3] that the long-time behaviour of most symmetric elementary rules ($F(r, s, t) = F(t, s, r)$) with the quiescent state ($F(0, 0, 0) = 0$) and with complex behaviour is similar to either rule 90 or rule 18, and can be fairly easily understood. The single notable exception (except for rule 54 for which is not clear whether it should be judged as 'complex') is rule 22. Indeed, it was shown in [4] that patterns produced by rule 22 show rather striking long-range correlations—striking since they are not visible to the naked eye and yet seem strong enough to make the specific entropy vanish.

0305-4470/87/124039+08$02.50

More precisely, let us denote by $p_N(s_1 \ldots s_N)$ the probability to find at some randomly chosen position a given string $S = \{s_1 \ldots s_N\}$ of length N in the asymptotic invariant distribution. The average information stored in this string is then

$$H_{N,1} = -\sum_{\{S\}} p_N(S) \log p_N(S). \tag{2}$$

The spatial block entropy $h_N^{(x)}$ is defined as

$$h_N^{(x)} = H_{N-1,1} - H_{N,1} \tag{3}$$

and the specific (spatial) entropy finally is $h^{(x)} = \lim_{N\to\infty} h_N^{(x)}$.

In the same way, one could define temporal or diagonal specific entropies by regarding the probability distribution for strings at fixed space points or strings $\{s_{i\pm t}(t)\}$. More natural from the dynamical systems point of view are temporal and diagonal block entropies not obtained from single strings but from rectangular resp rhombic blocks of spatial width N and temporal extent T. The temporal specific entropy is then defined [5] as

$$h^{(t)} = \lim_{N\to\infty} \lim_{T\to\infty} h_{N,T}^{(t)} \tag{4}$$

with

$$h_{N,T}^{(t)} = H_{N,T-1} - H_{N,T} \tag{5}$$

and the diagonal specific entropy analogous [6]. It is easily seen that for the diagonal entropies the N limit is already reached for $N = 2$, for all elementary rules. For the rules we are interested in, the same is true for the temporal entropies [4, 7], whence we shall consider only the case $N = 2$ in the following:

$$h^{(t)} = \lim_{T\to\infty} h_{2,T}^{(t)}. \tag{6}$$

The most striking result of [4] was that the block entropies $h_N^{(x)}$ and $h_{2,T}^{(t)}$ of rule 22 both seemed to converge algebraically to zero.

A somewhat less surprising but related result was found in [8] for the patterns generated by asymmetric rules of the structure

$$F(r, s, t) = r \,\mathrm{XOR}\, f(s, t). \tag{7}$$

It is easily seen that for all such rules one invariant distribution is completely random, i.e. $p_N(s, \ldots, s_N) = 1/2^N$ both for spatial strings at fixed time and for temporal strings at fixed position in space. Non-trivial spacetime patterns are generated by $f(s, t) = s$ OR t (rule 30), $f(s, t) = s$ OR NOT t (rule 45) and $f(s, t) = s$ AND t (rule 120), and by the rules obtained from these by exchanging 0 and 1. These patterns are shown in figure 1. What is not evident from figure 1 but is indicated by more extensive simulations [7] is that the random state is a unique attractor and is thus the most relevant state for these rules.

While there cannot be thus any long-range spatial correlations for rules of this type, it was found in [8] that temporal and diagonal block entropies show also algebraic convergence, although not to zero. Instead, the temporal block entropies seem to converge to the exact lower bound $h^{(t)} = 1$,

$$h_{2,T}^{(t)} \approx 1 + \text{constant}/T^{\alpha} \tag{8}$$

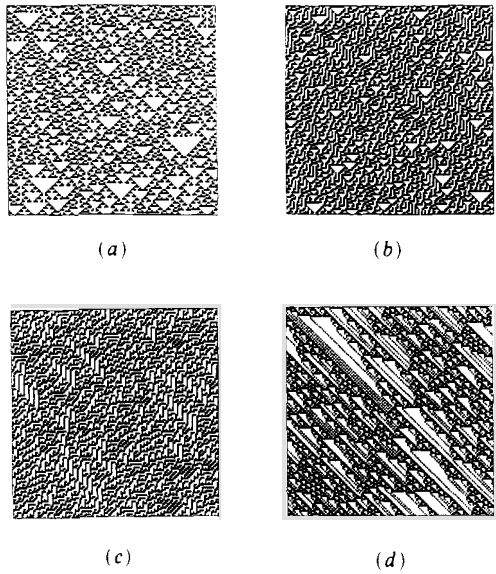

Figure 1. Parts of patterns created by rules 22(a), 30(b), 45(c) and 120(d) after random starts.

while the diagonal entropies along the diagonal $t = x + \text{constant}$ were compatible with an ansatz

$$h_{2,T}^{(+)} \approx h^{(+)} + \text{constant}/T^{\alpha} \tag{9}$$

with the same constant α but with $0 < h_{2,T}^{(+)} < 1$.

We had to use Monte Carlo simulations in order to see the algebraic entropy decay in rule 22. For rules 30, 45 and 120, on the other hand, exact enumerations were possible due to the fact that the invariant distribution is completely random. This has of course the advantage that no statistical errors are involved and one might hope to obtain better results by using sophisticated extrapolation techniques.

It is the purpose of this comment to report more enumerations. They concern primarily the temporal and diagonal entropies of rules 30, 45 and 120, but the trick used to make longer enumerations feasible is also applied in order to compute the density of '1' in patterns created by rule 22, T time steps after a random start. In all cases, we again found evidence for strong long-range correlations, and in the former cases we support the previous evidence for algebraic decays. But we also find very strong deviations from any simple behaviour, similar to that found for rule 22 in [4]. As a consequence, we were not able to make any substantial progress in estimating critical exponents.

Assume we want to estimate the probabilities for all rhombic blocks of width $N = 2$ and with some length T for rule 30, say. The straightforward way to do this consists in running through all 2^{2T} initial configurations of the spatial string of length $2T$ determining this block (see figure 2 for the case $T = 6$). Due to the complete randomness of the invariant measure, all these have the same weight, thus giving the required probabilities immediately. This was done in [8], but it becomes unpractical for $T > 12$ due to both storage and CPU time limitations (the results reported here demanded altogether ~5 h CPU time on a CDC CYBER 170/175).

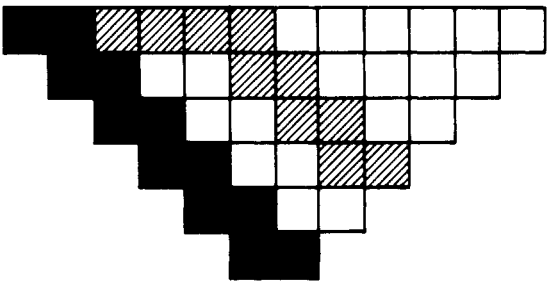

Figure 2. In order to estimate the probability for a configuration S on the block of size $2 \times T$ shown in black, one can enumerate all configurations starting from the first line. A faster algorithm enumerates all configurations starting from the domain shaded in grey.

The trick allowing longer enumerations is based on the observation that out of the 2^{2T} *a priori* possible block configurations only a small fraction occurs. Thus, it is much more efficient to enumerate, not initial configurations of spatial strings at constant time, but rather configurations on a combination of a rhombic block of length $T' < T$ and a short spatial string of length $2(T - T')$. Such a domain with $T' = 4$ is shaded in grey in figure 2. One has to know of course the possible configurations of length T' and their weights, but this can be done in the same way, using blocks of length $T'' < T'$, etc. This leads thus to a recursive evaluation of rhombic block configurations. Results obtained with $T' = T - 1$ are shown in table 1.

Once the rhombic block probabilities are known, they can be used to evaluate the probabilities of rectangular blocks needed for temporal entropies, for rules satisfying equation (7). The straightforward way of estimating these would again consist of evaluating all initial configurations on a spatial string of width $2T$ (see figure 3). This is considerably shortcut by enumerating instead configurations on the domain shaded in grey in figure 3, with results shown in table 2.

Table 1. Diagonal block entropies $h_{2,T}^{(+)}$ for rules 30, 45 and 120. The orientations of the blocks are as in figure 2.

T	Rule 30	Rule 45	Rule 120
1	2	2	2
2	1.155 639	1.155 639	1.155 639
3	1.090 018	0.922 180	0.860 488
4	1.026 493	0.900 554	0.740 154
5	0.956 246	0.886 629	0.675 540
6	0.904 710	0.824 482	0.613 245
7	0.867 407	0.786 809	0.572 954
8	0.842 178	0.766 299	0.549 768
9	0.821 049	0.741 097	0.527 908
10	0.802 548	0.716 884	0.508 334
11	0.787 901	0.699 700	0.486 023
12	0.774 669	0.686 505	0.471 577
13	0.763 143	0.673 892	0.461 366
14	0.753 519	0.661 258	0.451 027
15	0.744 128	0.650 274	0.441 830
16	—	0.640 065	0.434 135

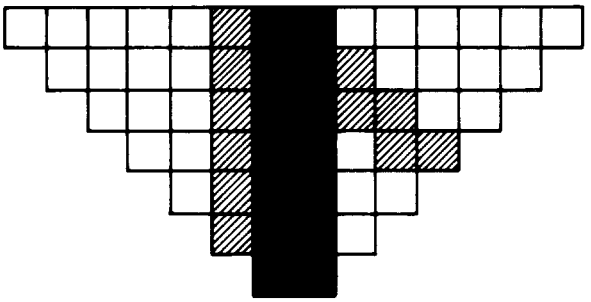

Figure 3. Same as figure 2 but for rectangular instead of rhombic blocks. An even better starting domain for enumerations consists of the right-hand part of the grey domain plus the left-hand black column.

Table 2. Temporal block entropies for rules 30, 45 and 120. The width of the blocks is $N = 2$.

T	Rule 30	Rule 45	Rule 120
1	2	2	2
2	1.5	1.5	1.5
3	1.327 820	1.327 820	1.327 820
4	1.295 009	1.250 000	1.263 105
5	1.272 318	1.228 477	1.200 468
6	1.252 210	1.213 131	1.166 892
7	1.232 916	1.196 145	1.146 228
8	1.215 303	1.183 207	1.127 558
9	1.202 200	1.171 430	1.111 934
10	1.189 036	1.161 035	1.099 634
11	1.178 823	1.151 941	1.090 168
12	1.169 031	1.143 791	1.082 152
13	1.161 467	1.136 776	1.075 578
14	1.154 363	1.130 359	1.069 855
15	1.148 627	1.124 744	1.064 674
16	1.143 428	1.119 710	1.060 035
17	1.138 938	1.115 137	1.055 972
18	—	1.110 994	1.052 382

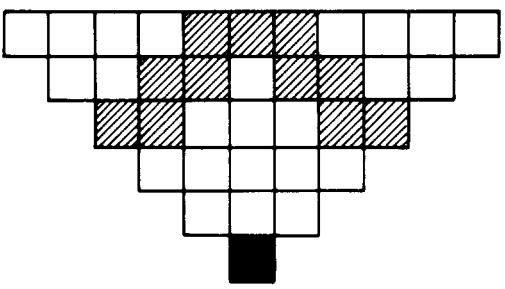

Figure 4. In order to estimate the density of '1' at the black site (i.e. after T iterations) one can enumerate all configurations starting from the shaded region, after having determined their weight.

Finally, if we want to estimate the density of '1' at finite times for rule 22, we can use as intermediate configurations those on the shaded domain in figure 4. Results are given in table 3.

Let us now discuss the results.

The shortest discussion applies to the results for rule 22. The decay of the density reflects the two-point correlation in timelike directions. Our present findings are in perfect agreement with the results for spatial correlations of [4]: there are long-range two-point correlations which decay neither like a power nor like an exponential. Instead, the decay is very irregular, and cannot be fitted by any simple ansatz. In order to show this, we plot in figure 5 the difference between the density after T iterations and the asymptotic density estimated in [4].

A more regular behaviour is found for the decay of block entropies. In figure 6, we show $h_{2,T}^{(r)} - 1$ on a doubly logarithmic scale. According to equation (8), we should expect straight lines with slope $-\alpha$. This is indeed roughly what is found, and we estimate

$$\alpha = \begin{cases} 0.62 \pm 0.08 & \text{(rules 30, 45)} \\ 1.11 \pm 0.04 & \text{(rule 120)} \end{cases} \tag{10}$$

where the quoted errors are just very crude subjective estimates. We have not performed a more sophisticated analysis since there are substantial deviations from equation (8), and it is not obvious how to take them into account.

The latter is even more true for the diagonal entropies. We show in figure 7 the differences $h_{2,T}^{(+)} - h_{2,T+1}^{(+)}$ on a log-log scale. According to equation (9), this time we

Table 3. Densities of '1' in patterns created by rule 22, after T iterations. The asymptotic Monte Carlo estimate is from [4].

T	Density of '1'
0	0.5
1	0.375
2	0.343 75
3	0.382 8125
4	0.361 3281
5	0.357 9102
6	0.354 8584
7	0.360 7483
8	0.356 3613
9	0.351 6407
10	0.356 0824
11	0.354 5738
12	0.355 2635
13	0.353 8610
14	0.353 8622
15	0.353 1522
16	0.353 4672
17	0.352 4912
18	0.352 8083
19	0.352 4303
20	0.352 5523
∞	0.350 96 ± 0.000 01

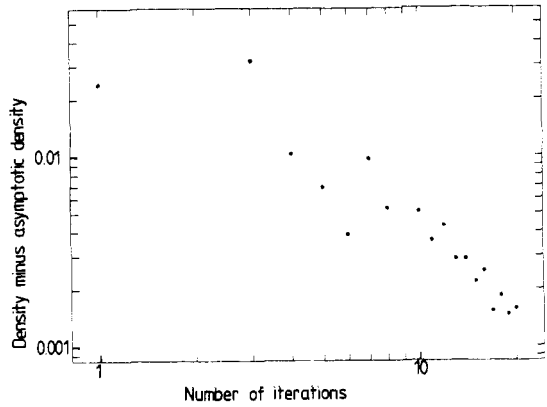

Figure 5. Difference between the density of '1' in rule 22 after T iterations and the asymptotic density.

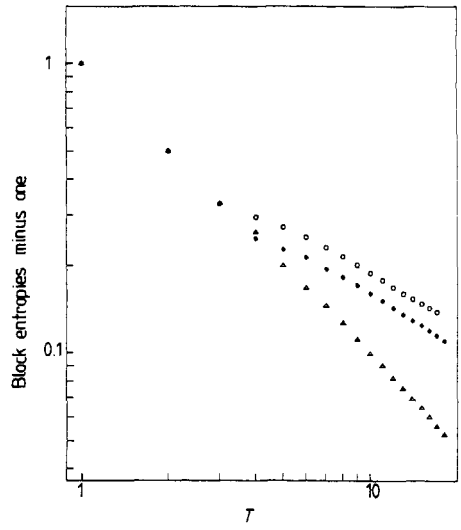

Figure 6. Temporal block entropies (in bits) minus 1, $h_{2,T}^{(t)}-1$, for rules 30 (circles), 45 (dots) and 120 (triangles), on a log-log scale. Equation (8) corresponds to a straight line with slope $-\alpha$.

should expect straight lines with slopes $-(1+\alpha)$. The data are clearly not in disagreement with this being the asymptotic behaviour, but the strong fluctuations render any detailed test impossible. If we accept equation (9), we estimate the diagonal entropies as

$$h^{(+)} \approx \begin{cases} 0.55 & \text{(rule 30)} \\ 0.45 & \text{(rule 45)} \\ 0.25 & \text{(rule 120).} \end{cases} \tag{11}$$

Both equations (10) and (11) are in agreement with [8]. Unfortunately, however, the errors estimated have not decreased as much as was expected, since the deviations from simple laws are stronger than foreseen. But we have no reason to doubt that the power laws hold asymptotically, since these deviations are not systematic.

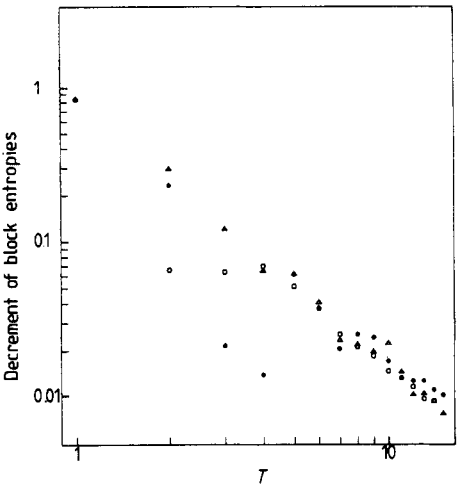

Figure 7. Decrements of diagonal block entropies, $h^{(+)}_{2,T} - h^{(+)}_{2,T+1}$, for rules 30 (circles), 45 (dots) and 120 (triangles). On the log-log scale used, a power-law convergence as in equation (9) would yield a straight line with slope $-(1+\alpha)$.

Summarising, we have again found evidence for strong long-range correlations for all four rules considered. Their structure seems simplest for rule 120 which seems the least complex of these rules. Entropies converge algebraically, while two-point correlations in rule 22 decay in a more complex fashion.

References

[1] von Neumann J 1966 *Theory of Self-reproducing Automata* ed A W Burks (Chicago, IL: University of Illinois Press)
Wolfram S 1986 *Theory and Applications of Cellular Automata* (Singapore: World Scientific)
[2] Wolfram S 1983 *Rev. Mod. Phys.* **55** 601
[3] Grassberger P 1983 *Phys. Rev.* A **28** 3666
[4] Grassberger P 1986 *J. Stat. Phys.* **45** 27
[5] Wolfram S 1984 *Physica* **10D** 1
[6] Milnor J 1984 *Institute of Advanced Study preprint*
Sinai Yu G 1985 *Commun. Math. Helv.* **60** 173
[7] Wolfram S 1986 *Adv. Appl. Math.* **7** 123
[8] Grassberger P 1986 *Int. J. Theor. Phys.* **25** 907